RECENT DEVELOPMENTS IN OPERATIONAL ATMOSPHERIC AND RADIOMETRIC CORRECTION OF HYPERSPECTRAL IMAGERY

Daniel Schläpfer[a/b], Rudolf Richter[c], and Andreas Hueni[a]

[a]Dept. of Geography/RSL, University of Zurich, Winterthurerstr. 190, 8057 Zürich, Switzerland,
daniel@rese.ch / ahueni@geo.uzh.ch
[b]ReSe Applications Schläpfer, Langeggweg 3, 9500 Wil, Switzerland,
[c]German Aerspace Center (DLR), D-82234 Wessling, Germany, rudolf.richter@dlr.de

ABSTRACT
With the advance of imaging spectroscopy systems, the correction of atmospheric influences has been continuously improved while adapting to the enhanced capabilities of current instruments. High resolutions airborne systems such as APEX, AISA, HYSPEX, and CASI-2/SASI have been developed, and powerful space systems such as ENMAP will soon be available. All these sensors promise high accuracy radiometric measurements and therefore require adequate and efficient pre-processing. This paper focuses on adaptations and improvements of the correction model and the software in order to cope with current and future imaging spectroscopy data. An idealized atmospheric correction scheme is proposed. It uses recent improvements for the automatic atmospheric water vapor retrieval, aerosol optical thickness and model determination, cirrus cloud detection and removal, cloud shadow correction, and adjacency correction as they are implemented in the ATCOR atmospheric correction model. The underlying MODTRAN database of look-up tables of radiative transfer calculations has been recompiled with a higher spectral resolution using the more accurate correlated-k algorithm in atmospheric absorption regions. Another enhancement is the adaptive correction of instrument spectral smile effects in combination with atmospheric correction in order to improve products uniformity. Last but not least, concepts and caveats for the integration of BRDF correction procedures and the integration of the respective spectral reference data are shown. Perspectives are outlined how reliable bi-hemispherical spectral albedo data products will be achieved in future preprocessing systems.

KEY WORDS: atmospheric correction, spectral uniformity, smile correction, water vapor, aerosol, topographic correction.

1. INTRODUCTION

The goal of atmospheric correction (AC) routines is an unambiguous characterisation of the surface reflectance properties. Currently available correction schemes include the ENVI ACM (formerly FLAASH, Adler-Golden et al. 1998) and ACORN (Analytic Imaging, 2001). Further systems which are not generally obtainable are the TAFKAA model for water applications (Gao et al., 2000), HATCH for hyperspectral spaceborne instruments (Qu et al., 2003), or the central data processing center (CDPC) at VITO (Biesemans et al., 2007).
The ATCOR model has been established as a standard state-of-the-art processing systems for multi- and hyperspectral imagery in the past years (Richter, 2009). Recent validation of its outputs reveals a high reliability of the processing for bottom of atmosphere reflectances, whereas the influence of surface BRDF effects is not considered in the current implementation (Schläpfer et al., 2008).

2. IDEALIZED METHOD FOR ATMOSPHERIC AND RADIOMETRIC CORRECTION

Ideally, an atmospheric and radiometric correction routine would result in bidirectional reflectance distribution functions (BRDFs) for all observed targets, as the BRDF is the unambigous radiometric property of the earth's surface (Nicodemus, 1977). Unfortunately, imaging spectrometers seldomly provide sufficient information to produce reliable BRDFs as most instruments acquire data for a single view geometry. Thus, a quantity not depending on the view geometry is of interest. The spectral albedo (i.e., the bi-hemispherical reflectance BHR) is a value which is well suited for an unbiased view of the earth's surface. Thus, it is the favorable output of atmospheric and radiometric processing.

2.1 Spectral albedo retrieval

The atmospheric correction tasks involve to the solution of the simplified radiative transfer equation for the derivation of bottom of atmosphere reflectance ρ (which is by its nature a hemispherical-directional reflectance quantity $HDRF_{meas}$).

$$\rho = HDRF_{meas} = \frac{\pi\left(L_S - L_{g,adj} - L_{atm}\right)\frac{1}{\tau_u}}{\tau_d E_0 \cos\varphi + E_{dif} s + E_{ter}} \quad , \qquad (1)$$

where:

- L_S calibrated at-sensor radiance
- $L_{g,adj}$ adjacency radiance
- L_{atm} atmospheric path radiance (single + multip. scattered)
- τ_u upward atmospheric transmittance
- τ_d downward atmospheric transmittance
- E_0 extraterrestrial solar irradiance (for the day of data acquisition)
- φ incidence angle on a tilted surface.
- E_{dif} hemispherical diffuse irradiance
- s skyview factor (visible portion of the sky; defined between 0 and 1)
- E_{ter} terrain irradiance, radiance incident directly from surrounding terrain slopes.

The derivation of spectral albedo from this reflectance value is the task of BRDF correction, which requires knowledge

about the BRDF of the target and the (diffuse) irradiance distribution. For operational use, an anisotropy factor needs to be calculated for each pixel, which accounts for the relation between measured hemispherical-directional reflectance $HDRF_{meas}$ and the spectral albedo (*BHR*), such that:

$$\rho_a = BHR = \frac{HDRF_{meas}}{K_{anif}}, \quad (2)$$

where the factor K_{anif} is found from an appropriate BRDF-model. If the influence of the diffuse irradiance component is included it may be derived as:

$$K_{anif} = \frac{BRF_{\text{model}} \cdot d + HDRF_{\text{model}} \cdot (1-d)}{BHR_{\text{model}}}, \quad (3)$$

where d is the portion of the direct irradiance. Eq. (3) assumes a homegeneous diffuse irradiance term which is also the irradiance term for a 'clean' $HDRF_{\text{model}}$ as defined by Nicodemus, (1977).

2.2 Implementation Scheme

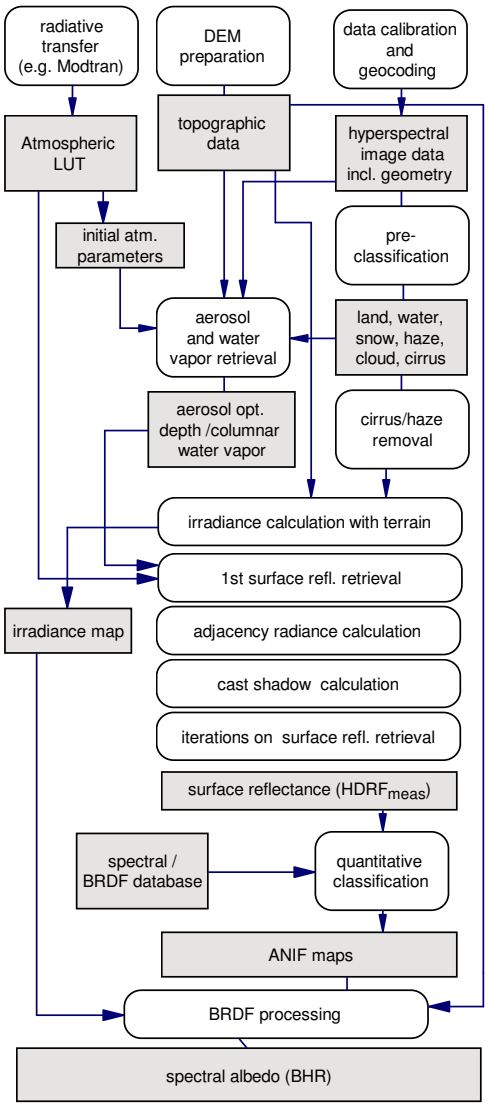

Figure 1: Complete atmospheric correction and radiometric normalization scheme.

Figure 1 shows a flow chart of a complete radiometric processing chain for hyperspectral data. Three major entities are required as input:

- atmospheric look-up-tables (LUTs) created using a radiative transfer code (e.g., Modtran) and some initial knowledge about the state of the atmosphere (e.g., aerosol model).
- digital elevation data and its derived quantities such as terrain slope, aspect, and skyview factor.
- calibrated and geocoded image data, stored in raw geometry including all geometric information (i.e., pixel location, solar and sensor geometry).

From this data, an automatic process is started. First the major land surface classes required for further processing are determined. Secondly, aerosol and water vapor parameters are calculated from the imagery. Cirrus and haze influences are then corrected in advance of any further processing using statistical approaches. All available input data are then used for the main atmospheric correction steps, which use an iterative approach for correction of terrain irradiance, adjacency effects, and cast shadow areas. This results in the bottom of atmosphere reflectance (i.e., the $HDRF_{meas}$).

The BRDF correction is a second phase in the processing which starts with the bottom-of-atmosphere reflectance. An estimate of the amount of the irradiance components is provided by the atmospheric correction part, whereas a quantitative classification of BRDF-relevant classes is made using a spectral reference database. Then the appropriate BRDFs can be appointed to the various classes, a prerequisite to the calculation of the desired spectral albedo product.

3. ASPECTS OF ATMOSPHERIC CORRECTION

The scheme as outlined in section 2 is a goal for AC schemes. In recent years, AC methods have been implemented for various sensor systems and as stand-alone software components. The ATCOR model is one of them which has been gradually improved and expanded toward this goal. Hereafter, an overview of example results based on this model is given and current pre-processing problems of hyperspectral airborne remote sensing are outlined.

3.1 LUT generation

The atmospheric LUTs contain the radiative transfer quantities required for the inversion of the at-sensor radiance to calculate the atmospheric parameters and surface reflectance. The corresponding parameter space typically comprises 5-7 dimensions (i.e., sensor view angle, solar zenith and azimuth angles, aerosol optical thickness, water vapor amount, ground elevation, wavelength, aerosol model). There are two basic ways of LUT generation:

a) LUTs are generated on the fly based on the image-specific atmospheric and geometric situation using the spectral band response functions.

b) A pre-compiled database of LUTs is provided covering the 5D to 7D parameter space, for the spectral range and resolution of all supported sensors

The first approach is used by the ENVI ACM and the VITO CDPC implementations of atmospheric correction, whereas ATCOR employs the second approach. The advantage of the first is the high flexibility for adaption to virtually any geometric situation and spectral resolution. The second

approach more easily allows (time-consuming) highest accuracy MODTRAN calculations (Berk et al., 1998): as an example, in current ATCOR releases the new correlated-k approach is used for increased accuracy in absorption bands. A drawback of the second approach is its fixed spectral resolution once the database has been compiled. Currently, an internal resolution of 0.6 nm is provided in the ATCOR database which suffices for instruments with spectral bandwidths of 3 nm and higher. This corresponds well with modern imaging spectrometers (such as AISA, HYSPEX, APEX, or CASI-2/SASI).

3.2 Topographic preparation

The calculation of terrain slope and aspect as well as the calculation of skyview factors can be done using straight-forward topographic modeling. With the advent of high spatial resolution imaging spectroscopy, this processing step has become more critical. Artifacts as depicted in Figure 2 may be avoided by simple spatial smoothing of coarse DEMs or by the use of DEMs at the very geometric accuracy as the imagery (e.g., acquired by laser scanning). However, at spatial resolutions down to 0.5m, the slope of surfaces can no longer be easily defined and no generic irradiance correction can be applied, e.g. in forests or settlements. New models for radiometric surface representation would be required but no generic solution is currently available.

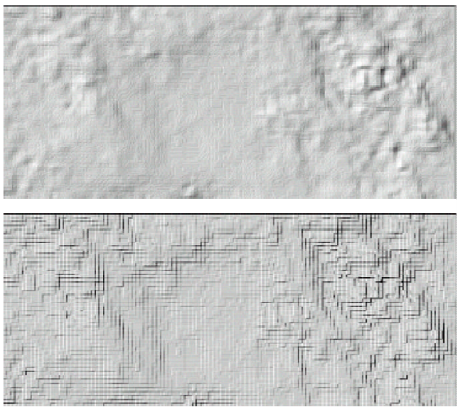

Figure 2 DEM artifacts on illumination map before (bottom) and after (top) post-processing.

3.3 Data calibration

Technical possibilities of sensor calibration have been vastly improved and allow for radiometric calibration of hyperspectral instruments down to the 2% level. Furthermore, inflight instabilities may be discovered using on-board calibration facilities such as in APEX (Itten et al., 2008). Therefore, we are now in the advantageous situation that airborne instruments may serve as calibration tools themselves and even help to improve radiative transfer codes. The efforts in the laboratory and facilities on board make relatively inacurate vicarious calibration approaches void and thus increase the reliability of the data.

3.4 Aerosol retrieval

The standard automatic method of aerosol optical thickness retrieval as proposed by Kaufman et al. (1997) works in areas with dark surfaces. In ATCOR, it was extended for automatic selection of standard aerosol models. Two main sources of error are still abundant: first, the spectral reflectance correlation factors between short-wave infrared (SWIR) and visible channels (vegation), or SWIR and NIR channel over water (Adler-Golden et al., 2005), especially for high spatial resolution instruments is uncertain and secondly, the abundance of dark objects highly depends on the surface cover type. Therefore, the correction is currently mostly done by standard values in non-vegetated areas. New methods are still under investigation for an aerosol characterisation over bright surfaces (Seidel et al., 2008).

3.5 Water vapor retrieval

The improved calibration and more reliable radiative transfer code simulations in absorption regions (as mentioned above) lead to water vapor retrieval results over land which are below the 5% limit in relative accuracy (Schläpfer et al., 1998). Over water, the water vapor retrieval is not yet feasible to a sufficient level of accuracy as only little ground reflected radiance is available. Therefore, an average water vapor amount is usually used for such data. An example based on independently simulated hyperspectral at-sensor radiances is given in Fig. 3. The variations of the retrieved water vapor over normal surfaces is within less than 3% for this example.

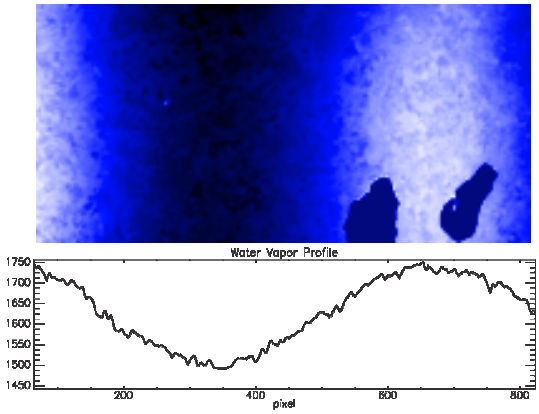

Figure 3 Water vapor retrieval results on simulated at sensor radiances and the corresponding spatial profile of water vapor (lakes are masked with an average value).

3.6 Cirrus and haze removal

Methods for haze removal based on image statistics are available for some years now and mostly work as expected on spatially variable surfaces.

Figure 4 Dehazing results on AVNIR-2 multispectral data.

For cirrus cloud removal, the 1.37 µm band has proven to provide accurate cirrus maps which can be used to remove cirrus effects from high altitude airborne or satellite imagery. Figure 4 shows an example of de-hazing of an AVNIR-2 scene.

3.7 Adjacency correction

The correction of the adjacency effect is of special importance to water applications but also is influencing all kind of land targets (Tanré et al., 1987). Current implementations use a spatial filter on the basis of a first order atmospheric correction to derive the adjacent area's apparent reflectance. This value is then used in conjunction with the aerosol scattering function and a spatial filter to remove the influence of adjacent reflectances onto the pixel's apparent surface reflecance value. An example based on SPOT multispectral satellite imagery is shown in Figure 5 below. The dynamics in the data are clearly reduced if no adjacency correction is used for this data, acquired at hazy conditions. Such strong effects mainly affect high altitude and satellite data, but even at flight altitudes down to 2 km, significant effects may be observed and need to be accounted for.

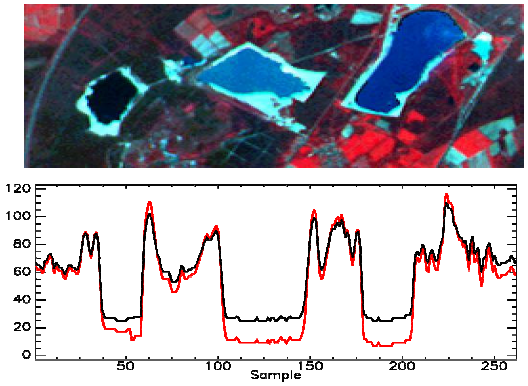

Figure 5 Adjacency correction in SPOT satellite imagery (20m resolution). Reflectance profile [% x 4] in NIR band: black line: no adjacency correction, red line: with adjacency correction.

3.8 Cloud and cast shadow correction

As the dynamics of airborne spectrometers has been improved significantly, the signal level in cast shadow and cloud shadow areas often is accurate enough to apply cloud shadow correction schemes. Current implementations use the statistics of the image to gain knowledge about the shadowed area in order to correct the 'darkening'. This routine is not suitable for data sets acquired below clouds as the complete statistics for intercomparison purpose is missing in these cases. So, the correction of airborne hyperspectral imagery under cloud cover remains a current research topic.

Figure 6 Deshadowing of a HYMAP scene near Munich.

3.9 Correction of spectral smile

Non-uniformities of imaging spectroscopy systems is a known problem which requires adequate processing (Nieke et al., 2008). Due to the spectral smile effect, the center wavelength of each channel changes with the across-track pixel position, and thus AC parameters will change too. Considerable efforts for an optimized coding are required to perform AC on a column-by-column basis within a reasonable time. Figure 7 shows an example of a naturally smooth sand spectrum retrieved from a simulated hyperspectral scene without and with smile correction. Large artifacts in the spectra appear in atmospheric absorption regions if a smile correction is neglected or if smile is corrected by linear interpolation only.

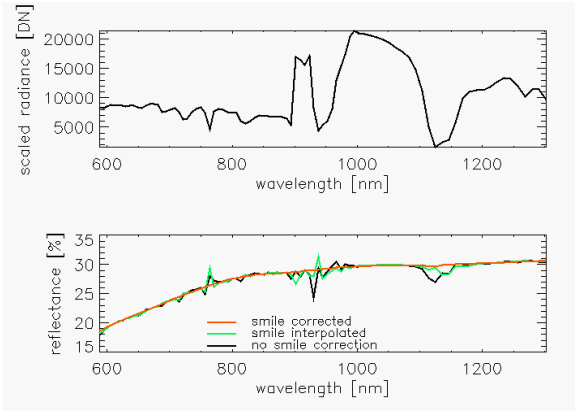

Figure 7 Original and processed sand spectrum without smile correction, with linear smile interpolation, and with columnar smile correction.

The correction of spectral smile has also significant influences on the water vapor retrieval routines (see Figure 8). Smile influences can only be remove if a columnar atmospheric correction is done.

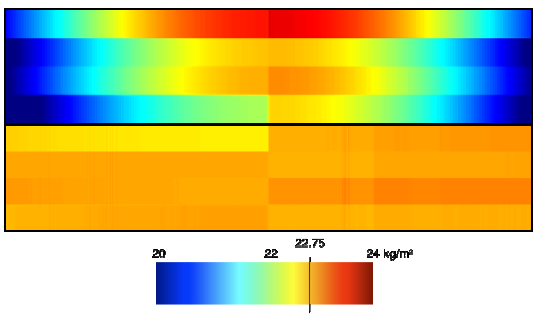

Figure 8 Water vapor retrieval over 8 different targets without smile correction (top), and with smile correction (bottom).

4. ASPECTS OF BRDF NORMALIZATION

Currently, no complete BRDF correction package is known to the authors which is applicable to single-view hyperspectral imagery. Therefore, efforts are taken to overcome this missing part of the processing chain. New tools shall therefore be developed for the correction of BRDF effects.

4.1 Empirical BRDF correction

BRDF effects are usually present in any kind of imagery, especially in mountainous terrain, as the local solar illumination angles varies with the slope and orientation of a surface element. Appropriate techniques to account for the non-Lambertian reflectance behavior are the Minnaert and C correction methods (Riano et al., 2003) and are to be corrected accordingly. The succesful removal of topographic effects mainly depends on the quality of the DEM, the DEM resolution with respect to the sensor's footprint, and the accuracy of the orthorectification. Figure 9 presents an example of an empirical topographic correction with the empirical BRDF correction approach of ATCOR. Most topographic features are adequately corrected in the example as the used generic BRDF function accounts empirically for typical non-Lambertian characteristics of the surface due to variations of the incidence angle in terrain. However, object-specific differences are not accounted for.

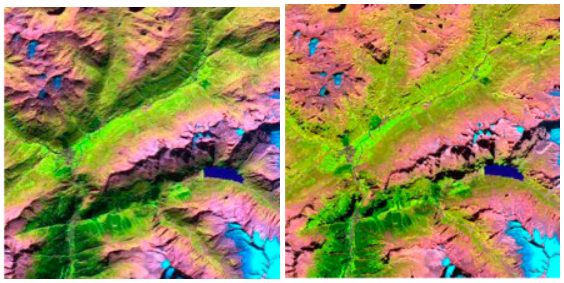

Figure 9 Empirical BRDF correction in rugged terrain. SPOT-5 scene, left: original data, right after correction.

4.2 BRDF-model based correction process

Figure 10 Results of BRDF correction using measured BRDF values (top: corrected image, bottom: anisotropy factor for the lawn object).

If the appropriate correction function can be assigned to each image pixel, the image correction can take place. It uses the information of the irradiance as well as the BRDF parameter. An anisotropy factor K_{anif} is defined as decribed in Eq. (3). In terrain, the slope of the terrain may strongly influence the results. Thus, K_{anif} needs to be adjusted – at least for objects void of vertical structures – such that the BRDF is tilted against the horizontal direction. In this way, adjusted K_{anif} functions are derived. The correction itself is then performed using Eq. (4). A sample result of the process is given in Figure 10, where the anisotropy is corrected for a lawn target in the test image near Munich. More details about this procedure can be found in Feingersh et al. (2009).

4.3 Spectral classification

Automatic classification is required at two stages of atmospheric and radiometric correction. First, it is used as a pre-classification for the subsequent steps of aerosol and water vapor retrieval as well as haze and cirrus detection and removal. A more accurate classification is required as a starting point for a BRDF correction routine. Ideally, this classification should be quantitative in order to allow mixtures of classes and avoid discontinuities in the data processing. Figure 11 shows an example of the ATCOR default classification with vegetation classes coded in different colors of green, water (blue), soils (brown), and sand, asphalt (grey).

Figure 11 Automatic coarse spectral classification of a HYMAP scene.

4.4 BRDF reference

A spectral database needs to be provided to gain access to valid BRDFs in conjunction to the imagery. The BRDFs held by the database may be either retrieved from goniometer measurements in the field/laboratory or created by BRDF models. A comprehensive metadata model must describe the spectral data in order to support data selection based on metadata queries. The spectral database system SPECCHIO

is planned to be used as a basis for the development of such a reference database (Hueni et al., 2009a/b). The data held by the reference database needs to be strictly controlled and a 'Spectral reference generator' is used to move data from the generic SPECCHIO database to the reference database (see Figure 12).

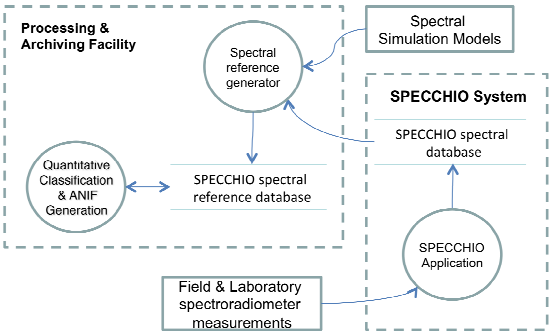

Figure 12 Dataflow within the processing and archiving facility and an external spectral database.

5. CONCLUSIONS AND OUTLOOK

Current achievements and problems of atmospheric correction have been outlined. In the past years, quite some progress was made with respect to spectral calibration, haze and cloud correction, aerosol and water vapor retrieval, as well as adjacency correction. More recent advances are the columnar correction of spectral smile and higher resolutions of the atmospheric databases. For a complete atmospheric processing chain, some critical elements are still missing and need to be addressed or improved in future developments:

- aerosol retrieval over bright objects,
- water vapor retrieval over dark objects,
- uniformisation of smile and frown effects,
- topographic processing of high resolution imagery,
- empirical and class-specific BRDF correction,

This will lead to the generation of spectral albedo products from single-geometry observations as the standard product of atmospheric and radiometric correction.

ACKNOWLEDGEMENTS

We acknowledge specifically Luis Guanter from GFZ Potsdam for providing simulated sample data, Tobias Kellenberger from Swisstopo, Bern for the SPOT sample imagery, Tal Feingersh from University of Tel Aviv for providing the BRDF correction sample. Last but not least Prof. Klaus I. Itten is grealty acknowledged for his continued support of these developments.

REFERENCES

S.M. Adler-Golden, A. Berk, L.S. Bernstein, and S. Richtsmeier, 1998: FLAASH, a MODTRAN4 atmospheric correction package for hyperspectral data retrievals and simulations, in *Proc. Summaries 7th JPL Airborne Earth Sci. Workshop*, pp. 1-9.

S.M. Adler-Golden, P.K. Acharya, A. Berk, M.W. Matthew, and D. Gorodetzky, 2005: *Remote bathymetry of the littoral zone from AVIRIS, LASH, and QuickBird imagery*, IEEE TGARS, 43:337-347.

Analytic Imaging, 2001: *"ACORN", Atmospheric correction now – version 3.12*, Analytical Imag. Geophys. LLC, Boulder, CO.

A. Berk, L.S. Bernstein, G. P. Anderson, K. Acharya, D. C. Robertson, J. H. Chetwynd, and S. M. Adler-Golden, 1998: *MODTRAN cloud and multiple scattering upgrades with application to AVIRIS*, Remote Sens. Environ., 65:367-375.

J. Biesemans, Sterckx, S., Knaeps, E., Vreys, K., Adriaensen, S., Hooyberghs, J., Meuleman,K., Kempeneers, P., Deronde B., Everaerts, J., Schläpfer, D. And Nieke, J., 2007, Image processing workflows for airborne remote sensing. In *5th EARSeL SIG Imaging Spectroscopy Workshop*, 23-25 April 2007, Bruges, Belgium. pp. 14.

T. Feingersh, D. Schläpfer, E. Ben-Dor, 2009: BREFCOR - Towards operational BRDF correction for imaging spectrometry data, *Proc. 6th Earsel Workshop on Imaging Spectroscopy*, this issue, pp.6.

B.-C. Gao, M. J. Montes, Z. Ahmad, and C. O. Davis (2000), Atmospheric Correction Algorithm for Hyperspectral Remote Sensing of Ocean Color from Space, *Applied Optics,* 39(6):887-994.

A. Hueni, Biesemans, J., Meuleman, K., Dell'Endice, F., Schläpfer, D., Adriaensen, S., et al., 2009. Structure, Components and Interfaces of the Airborne Prism Experiment (APEX) Processing and Archiving Facility. *IEEE TGARS,* 47(1):29-43.

A. Hueni, Nieke, J., Schopfer, J., Kneubühler, M. & Itten, K., 2009. The spectral database SPECCHIO for improved long term usability and data sharing. *Computers & Geosciences,* 35(3):557-565.

K.I. Itten, F. DellEndice, A. Hueni, M. Kneubühler, D. Schläpfer, D. Odermatt, F. Seidel, S. Huber, J. Schopfer, T. Kellenberger, Y. Bühler, P. D'Odorico, J. NIeke, E. Alberti, K. Meuleman, 2008: *APEX - the Hyperspectral ESA Airborne Prism Experiment*, Sensors vol. 8 pp. 6235-6259, http://dx.doi.org/10.3390/s8106235.

Y.J. Kaufman, A. E. Wald, L. A. Remer, B.-C. Gao, R.-R. Li, and L. Flynn, 1997: *The MODIS 2.1 µm channel – correlation with visible reflectance for use in remote sensing of aerosol*, IEEE TGARS Vol. 35:1286-1298.

F.E. Nicodemus, J.C. Richmond, J. J. Hsia, I.W Ginsberg, and T Limperis, 1977: *Geometrical Considerations and Nomenclature for Reflectance.* National Bureau Of Standards, U.S. Department of Commerce, Washington D.C. 20234, pp. 52.

J Nieke, D. Schläpfer, F. DellEndice, J. Brazile, and K. I. Itten, 2008: *Uniformity of Imaging Spectrometry Data Products.* IEEE TGARS, 46(10):3326 - 3336.

Z. Qu, B. C. Kindel, and A.F.H. Goetz, 2003: *The High Accuracy Atmospheric Correction for Hyperspectral Data (HATCH)* Model," IEEE TGARS, 41:1223-1231.

D. Riano, E. Chuvieco, J. Salas, and I. Aguado, 2003: *Assessment of different topographic corrections in Landsat TM data for mapping vegetation types*" IEEE TGARS, 41:1056-1061.

R. Richter, 2009: *Atmospheric / Topographic Correction for Airborne Imagery* (ATCOR-4 User Guide, Version 5.0). DLR-IB 565-02/09, pp. 145.

D. Schläpfer, J. Biesemans, A. Hueni, and K. Meuleman, 2008: *Evaluation of the Atmospheric Correction Procedure for the APEX Level 2/3 Processor*. In: Remote Sensing of Clouds and the Atmosphere XIII, Proc. SPIE 7107, http://dx.doi.org/10.1117/12.799884, pp 12.

D. Schläpfer, C. C. Borel, J. Keller, and K.I. Itten, 1998: *Atmospheric precorrected differential absorption technique to retrieve columnar water vapor*, Remote Sens. Environ., Vol. 65, 353-366.

F. Seidel, D. Schläpfer, J. Nieke, K. I. Itten, 2008: *Sensor Performance Requirements for the Retrieval of Atmospheric Aerosols by Airborne Optical Remote Sensing*. Sensors, vol. 2008 (8):1901-1914.

D. Tanré, P.Y. Deschamps, P. Duhaut, and M. Herman, 1987: *Adjacency Effect Produced by the Atmospheric Scattering in Thematic Mapper Data.* Journal of Geophysical Research Vol. 92(D10): 12.000 - 12.006.